LABORATORY TESTS ASSESSING THE EFFECTIVENESS OF THE NF-FF TRANSFORMATION WITH HELICOIDAL SCANNING FOR ELECTRICALLY LONG ANTENNAS

F. D'Agostino, F. Ferrara, C. Gennarelli, R. Guerriero and M. Migliozzi

Dipartimento di Ingegneria dell'Informazione ed Ingegneria Elettrica
University of Salerno
via Ponte Don Melillo, Fisciano (Salerno) 84084, Italy

Abstract—This paper deals with the experimental validation of an effective near-field-far-field transformation technique with helicoidal scanning particularly suitable for electrically long antennas, whose validity has been numerically assessed in a previous authors' paper. Such a technique relies on the results relevant to the nonredundant sampling representations of the electromagnetic fields and makes use of an optimal sampling interpolation algorithm, which allows the reconstruction of the near-field data needed by the near-field-far-field transformation with cylindrical scan. The use of a prolate ellipsoid instead of a sphere to model an elongated antenna allows one to consider measurement cylinders with a diameter smaller than the antenna height, thus reducing the error related to the truncation of the scanning zone. Moreover, a significant reduction of the needed near-field data is also obtained. The comparison of the far-field patterns reconstructed from the acquired helicoidal measurements with those obtained from the data directly measured on the classical cylindrical grid assesses the effectiveness of the near-field-far-field transformation using this innovative scanning technique. At last, its validity is further confirmed by the very good agreement with the direct far-field measurements.

Corresponding author: C. Gennarelli (gennar@diiie.unisa.it).

1. INTRODUCTION

Measurement techniques in the antenna near-field (NF) region play a significant role in the evaluation of far-field (FF) patterns and in the determination of electrical and/or geometrical properties [1]. In particular, the pattern evaluation from NF measurements allows one to overcome those drawbacks which, for electrically large radiating sources, make it unpractical to measure the FF data on a conventional FF range.

Nowadays, the reduction of the time required for the acquisition of the NF data is becoming a very important issue for the antenna measurement people. In fact, such a time is currently very much greater than that needed to carry out the corresponding NF-FF transformation. In this framework, innovative NF-FF transformation techniques from a nonredundant number of data collected along spirals wrapping the conventional scanning surfaces have been recently developed [2–7]. They have been implemented, as suggested by Rahmat-Samii et alii in [8], by means of continuous and synchronized movements of the positioning systems of the probe and antenna under test (AUT). In particular, an effective NF-FF transformation with helicoidal scanning has been proposed in [3, 7]. It relies on the theoretical results concerning the nonredundant sampling representations of the electromagnetic (EM) fields [9] and makes use of the optimal sampling interpolation (OSI) expansions [10, 11]. Accordingly, the NF data needed by the classical NF-FF transformation with cylindrical scanning [12] can be reconstructed by interpolating the nonredundant ones acquired on the helix. The required two-dimensional algorithm has been obtained [7]: a) By assuming the AUT enclosed in the smallest sphere able to contain it; b) by developing a nonredundant sampling representation of the voltage on the helix; c) by choosing the helix step equal to the sample spacing required to interpolate the data along a generatrix.

As explicitly pointed out in [13, 14], the use of the spherical AUT modelling is not very effective when considering electrically long antennas, i.e., those having a predominant dimension, such as the radiating systems for radio base stations. As a matter of fact, it does not permit to consider measurement cylinders with a radius smaller than one half the antenna maximum size, thus reflecting in an increase of the error related to the truncation of the scanning surface. Moreover, due to its "volumetrical" redundancy, it gives rise to an increase in the number of the NF data. Quite analogous drawbacks occur in the planar spiral scanning when dealing with quasi-planar antennas having two dimensions greater than the third

one [14, 15]. NF-FF transformation techniques with helicoidal and planar spiral scannings, which do not exhibit the above mentioned constraint on the measurement surface distance, have been recently proposed in [16, 17], respectively. However, these approaches require a large number of NF data, since they do not rely on the nonredundant sampling representations.

On the other hand, the advantages in using spheroidal volume support regions when considering elongated or flat sources has been highlighted in [18], although in a different framework.

In order to overcome the above drawbacks, an efficient NF-FF transformation technique with helicoidal scanning tailored for elongated antennas has been recently proposed in [13], by assuming the AUT as enclosed in a prolate spheroid, a shape particularly suitable to deal with such a kind of antennas, but which remains quite general and contains the spherical modelling as particular case. The use of an oblate ellipsoid has been proposed in [15] to get a NF-FF transformation with planar spiral scanning suitable for quasi-planar antennas. Then, a unified theory of the spiral scannings for nonspherical antennas has been developed in [14] by properly extending that using the spherical AUT modelling [7]. To this end, an AUT with one or two predominant dimensions is no longer considered as enclosed in a sphere, but in a proper convex domain bounded by a rotational surface. It has been so proved that the voltage acquired by a nondirective probe can be reconstructed on a quite arbitrary rotational surface from a nonredundant number of its samples lying on a proper spiral wrapping it. The only required condition is that the surface is obtained by rotating a meridian curve always external to the cone tangent to the surface modelling the AUT and having the vertex at the observation point.

The goal of this paper is to experimentally assess the effectiveness of the NF-FF transformation technique with helicoidal scanning for electrically long antennas [13]. The experimental validation has been carried out both at the laboratory of antenna characterization of the University of Salerno, where an advanced cylindrical NF measurement facility supplied by MI Technologies is available, and at the anechoic chamber of the University of Naples "Parthenope", provided with a FF measurement range.

2. VOLTAGE RECONSTRUCTION FROM NONREDUNDANT HELICOIDAL SAMPLES

The main results [13] concerning the reconstruction of the voltage from a nonredundant number of its samples collected by the measurement

probe along a helix are reported in the following.

Let us consider an electrically long AUT and a probe scanning a proper helix lying on a cylinder of radius d (see Fig. 1) and adopt the spherical coordinate systems (r, ϑ, φ) and (R, Θ, Φ) for denoting an observation point in the NF and FF region, respectively. As shown in [19], the voltage V measured by a non directive probe has the same effective spatial bandwidth of the field, accordingly, the nonredundant sampling representation of EM fields can be applied to it. As a consequence, by assuming the AUT as enclosed in a convex domain bounded by a surface Σ with rotational symmetry and describing the observation curve by a proper analytical parameterization $\underline{r} = \underline{r}(\eta)$, the probe "reduced voltage" $\tilde{V}(\eta) = V(\eta)e^{j\psi(\eta)}$, $\psi(\eta)$ being a phase function to be determined, can be approximated by a spatially bandlimited function. The corresponding bandlimitation error becomes negligible as the bandwidth exceeds a critical value W_η [9]. Therefore, such an error can be effectively controlled by choosing a bandwidth equal to $\chi' W_\eta$, χ' being an excess bandwidth factor slightly greater than unity for an electrically large AUT.

When considering a long AUT, it is no longer convenient to adopt the smallest sphere [7] as surface Σ enclosing it, but, as suggested in [13, 14], the smallest prolate ellipsoid having major and minor semi-axes equal to a and b (Fig. 1).
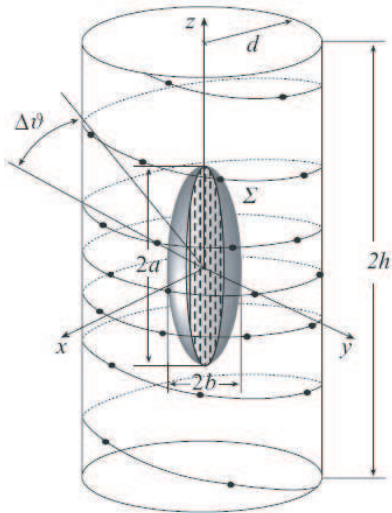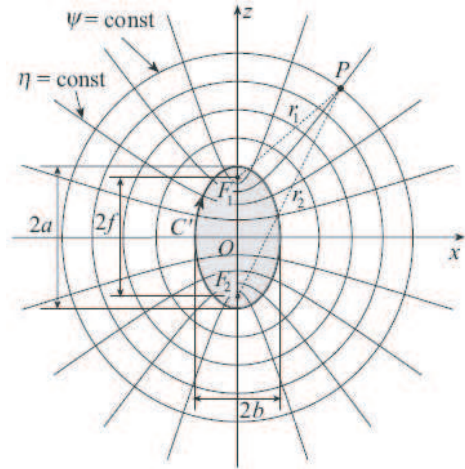

Figure 1. Helicoidal scanning.

Figure 2. Curves $\psi = $ const and $\eta = $ const.

The unified theory of spiral scannings for nonspherical antennas [14], obtained by paralleling the corresponding rigorous procedure valid when adopting the spherical AUT modelling [7], allows one to develop the voltage representation on the cylinder from a nonredundant number of its samples collected on the helix. To this end, it is necessary: a) To determine a nonredundant representation along the helix; b) to choose the step of the helix such that it intersects any generatrix at points having the sample spacing needed for the interpolation. In particular, according to [13, 14], the bandwidth W_η and parameterization η relevant to a generatrix, and the corresponding phase function ψ are given by

$$W_\eta = \frac{4a}{\lambda} E\left(\pi/2 | \varepsilon^2\right) \tag{1}$$

$$\psi = \beta a \left[v \sqrt{\frac{v^2 - 1}{v^2 - \varepsilon^2}} - E\left(\cos^{-1} \sqrt{\frac{1 - \varepsilon^2}{v^2 - \varepsilon^2}} \Big| \varepsilon^2 \right) \right] \tag{2}$$

$$\eta = (\pi/2) \left[1 + E(\sin^{-1} u | \varepsilon^2) / E(\pi/2 | \varepsilon^2) \right] \tag{3}$$

where λ is the wavelength, β the wavenumber, $u = (r_1 - r_2)/2f$ and $v = (r_1 + r_2)/2a$ are the elliptic coordinates, $r_{1,2}$ being the distances from observation point P to the foci and $2f$ the focal distance of C', intersection curve between a meridian plane and Σ. Moreover, $\varepsilon = f/a$ is the eccentricity of C' and $E(\cdot|\cdot)$ denotes the elliptic integral of second kind. Note that in any meridian plane the curves $\psi = \text{const}$ and $\eta = \text{const}$ are ellipses and hyperbolas confocal to C' (Fig. 2).

According to [14], the helix can be obtained by projecting on the scanning cylinder a proper spiral wrapping the ellipsoid. The helix step, determined by two consecutive intersections with a given generatrix, is equal to the sample spacing $\Delta\eta = 2\pi/(2N'' + 1)$ needed to interpolate the voltage along a generatrix. Note that $N'' = \text{Int}(\chi N') + 1$, where $\text{Int}(x)$ denotes the integer part of x, $N' = \text{Int}(\chi' W_\eta) + 1$ and $\chi > 1$ is an oversampling factor needed to control the truncation error. The projection is obtained via the curves at $\eta = \text{const}$ (see Fig. 2). Accordingly, the parametric equations of the helix, when imposing its passage through a fixed point Q_0 of the generatrix at $\varphi = 0$, are:

$$\begin{cases} x = d\cos(\phi - \phi_i) \\ y = d\sin(\phi - \phi_i) \\ z = d\cot[\vartheta(\eta)] \end{cases} \tag{4}$$

wherein ϕ is the angular parameter describing the helix, ϕ_i is the value of ϕ at Q_0, and $\eta = k\phi$, k being a parameter related to the helix step by $k = 2\pi/\Delta\eta$. Accordingly, $k = 1/(2N'' + 1)$.

The parameter ξ and phase factor γ to get a nonredundant representation of the voltage along the helix can be again determined by applying the unified theory [14]. In particular, ξ is β/W_ξ times the arclength of the projecting point on the spiral wrapping Σ and γ coincides with the phase function ψ relevant to a generatrix. Moreover, W_ξ is chosen equal to β/π times the length of the spiral wrapping the ellipsoid from pole to pole.

In light of the above results, the reduced voltage at any point Q of the helix can be recovered via the OSI expansion [13, 14]:

$$\tilde{V}(\xi) = \sum_{m=m_0-p+1}^{m_0+p} \tilde{V}(\xi_m)\,\Omega_M\,(\xi-\xi_m)\,D_{M''}\,(\xi-\xi_m) \qquad (5)$$

where $2p$ is the number of retained samples $\tilde{V}(\xi_m)$, $m_0 = \mathrm{Int}[(\xi - \xi(\phi_i))/\Delta\xi]$ is the index of the sample nearest (on the left) to Q, and

$$\xi_m = \xi(\phi_i) + m\Delta\xi = \xi(\phi_i) + 2\pi m/\left(2M''+1\right) \qquad (6)$$

with $M'' = \mathrm{Int}(\chi M') + 1$ and $M' = \mathrm{Int}(\chi' W_\xi) + 1$. Moreover,

$$D_{M''}(\xi) = \frac{\sin((2M''+1)\xi/2)}{(2M''+1)\sin(\xi/2)};$$

$$\Omega_M(\xi) = \frac{T_M\left[-1 + 2\left(\cos(\xi/2)/\cos\left(\bar{\bar{\xi}}/2\right)\right)^2\right]}{T_M\left[-1 + 2/\cos^2\left(\bar{\bar{\xi}}/2\right)\right]} \qquad (7)$$

are the Dirichlet and Tschebyscheff Sampling functions, wherein $T_M(\xi)$ is the Tschebyscheff polynomial of degree $M = M'' - M'$ and $\bar{\bar{\xi}} = p\Delta\xi$.

Expansion (5) can be properly employed to evaluate the voltage at any point P on the cylinder and, in particular, at those required to carry out the classical NF-FF transformation with cylindrical scanning [12]. In fact, it allows the evaluation of the "intermediate" samples, namely the voltage values at the intersection points of the helix with the generatrix passing through P. Once these samples have been determined, because of the particular choice of $\Delta\eta$, the reduced voltage at P and can be reconstructed via the following OSI expansion:

$$\tilde{V}(\eta(\vartheta),\varphi) = \sum_{n=n_0-q+1}^{n_0+q} \tilde{V}(\eta_n)\Omega_N(\eta-\eta_n)D_{N''}(\eta-\eta_n) \qquad (8)$$

wherein $N = N'' - N'$, $n_0 = \mathrm{Int}[(\eta-\eta_0)/\Delta\eta]$, $2q$ is the number of the retained intermediate samples $\tilde{V}(\eta_n)$, and

$$\eta_n = \eta_n(\varphi) = \eta(\phi_i) + k\varphi + n\Delta\eta = \eta_0 + n\Delta\eta \qquad (9)$$

3. LABORATORY TESTS

Some experimental results assessing the validity of the described NF-FF transformation technique with helicoidal scanning are shown in this section.

The experimental tests have been carried out in the anechoic chamber available at the laboratory of antenna characterization of the University of Salerno, which is provided with a NF facility system supplied by MI Technologies. This chamber, whose dimensions are $8\,\mathrm{m} \times 5\,\mathrm{m} \times 4\,\mathrm{m}$, is covered with pyramidal absorbers ensuring a background noise lower than $-40\,\mathrm{dB}$. A vertical scanner and a rotating table allow one to acquire the NF data at any point on a cylindrical surface surrounding the AUT. The rotating table MI-6111B, mounted with its rotary axis parallel to the vertical scanner, ensures an angular precision of $\pm 0.05°$, whereas the vertical scanner, whose height is 240 cm, is characterized by a linear precision of ± 0.005 cm. The controller MI-4190, connected to a host computer by means of a IEEE-488 interface, is used to control the positioners motion and is completed by the option MI-4193, so that it is able to simultaneously drive both the positioners. The amplitude and phase measurements are performed by means of a vectorial network analyzer Anritsu 37247C. This last is computer-controlled and is characterized by wide dynamic range, high sensitivity and linearity over the range from 40 MHz to 20 GHz. An open-ended MI-6970-WR90 rectangular waveguide is used as probe.
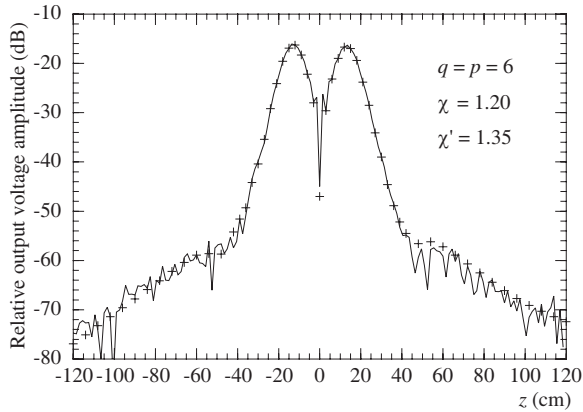
The AUT, located in the plane $x = 0$, is a very simple H-plane
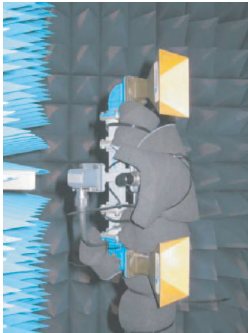
Figure 3. Photo of the monopulse antenna.
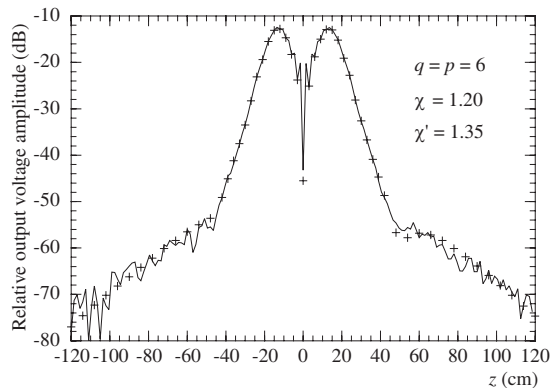
Figure 4. Amplitude of the probe voltage on the generatrix at $\varphi = 0°$. Solid line: Measured. Crosses: Interpolated.
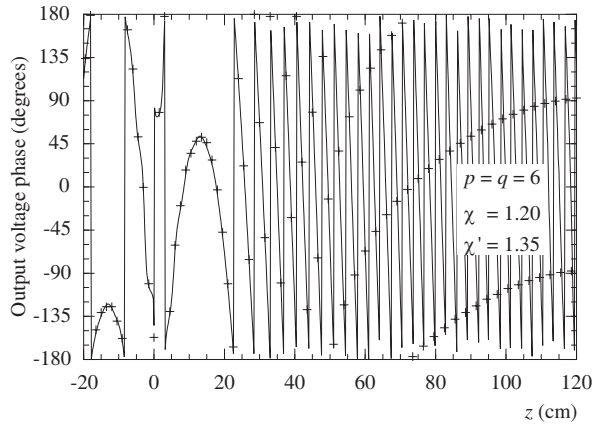
Figure 5. Amplitude of the probe voltage on the generatrix at $\varphi = 30°$. Solid line: Measured. Crosses: Interpolated.

monopulse antenna, operating at $10\,\mathrm{GHz}$ in the difference mode. It has been realized (Fig. 3) by using two pyramidal horns ($8.9 \times 6.8\,\mathrm{cm}$) made by Lectronic Research Labs at a distance of $26\,\mathrm{cm}$ (between centers) and a hybrid Tee. According to the previously described representation, the AUT has been modelled as enclosed in a prolate ellipsoid with major and minor semi-axes equal to $27\,\mathrm{cm}$ and $5\,\mathrm{cm}$. The probe voltages have been collected on a helix lying on a cylinder with $d = 16.6\,\mathrm{cm}$ and $2h = 240\,\mathrm{cm}$.

To assess the effectiveness of the two-dimensional OSI algorithm, the amplitudes of the reconstructed probe voltage relevant to the generatrices at $\varphi = 0°$ and $\varphi = 30°$ are compared in Figs. 4 and 5 with those directly measured on the same generatrices. As can be seen, the reconstructions are everywhere very good, save for the peripheral zone (below about $-60\,\mathrm{dB}$). It is worthy to note that a smoother behaviour of the reconstructed voltage with respect to the measured one results, since the spatial harmonics relevant to the noise sources outside the AUT spatial bandwidth are cut away for the filtering properties of the interpolation functions. For completeness, the comparison between the phase of the recovered voltage and the measured one on the generatrix at $\varphi = 0°$ is shown in Fig. 6 only in the range $[-20\,\mathrm{cm}, 120\,\mathrm{cm}]$ to improve its readability. Note that all the reported reconstructions have been obtained by using $\chi' = 1.35$, $\chi = 1.20$, and $p = q = 6$.

The overall effectiveness of the described NF-FF transformation is assessed by comparing the H-plane FF pattern reconstructed from the acquired helicoidal NF data with that obtained from the data directly measured on the classical cylindrical grid. In both the cases, the software package MI-3000 has been used to get the FF reconstructions.

Figure 6. Phase of the probe voltage on the generatrix at $\varphi = 0°$. Solid line: Measured. Crosses: Interpolated.
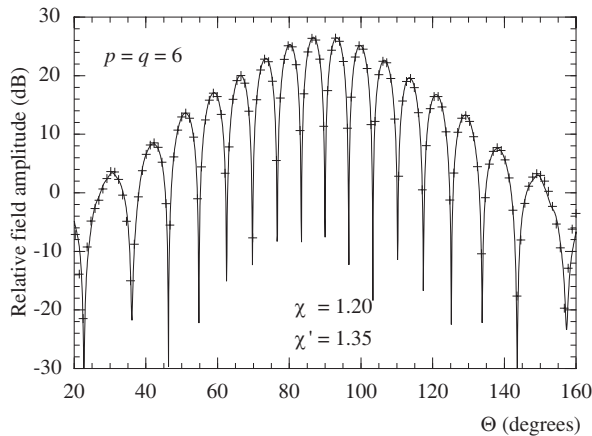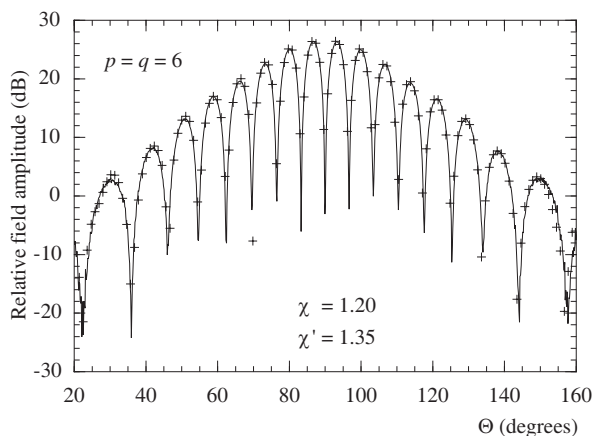

Figure 7. H-plane pattern. Solid line: Reference. Crosses: Reconstructed from NF data acquired via helicoidal scanning.

Obviously, the two-dimensional OSI algorithm has been employed for recovering the cylindrical data needed to perform the NF-FF transformation from the acquired helicoidal ones. As can be seen (Fig. 7), also in such a case, there is a very good agreement, thus confirming the effectiveness of the approach.

Moreover, the H-plane pattern obtained from helicoidal measurements is compared in Fig. 8 with that directly measured at the anechoic

chamber of the University of Naples "Parthenope", provided with a FF measurement range. As can be seen, although the measurements have been carried out with quite different techniques and environmental conditions, a very good agreement results, save for small discrepancies in the far-out side lobes region, due to the truncation of the scan zone.

The following figures are relevant to the same monopulse antenna when operating in the sum mode. In particular, Figs. 9 and 10 refer to the comparison E and H-planes FF patterns reconstructed from the
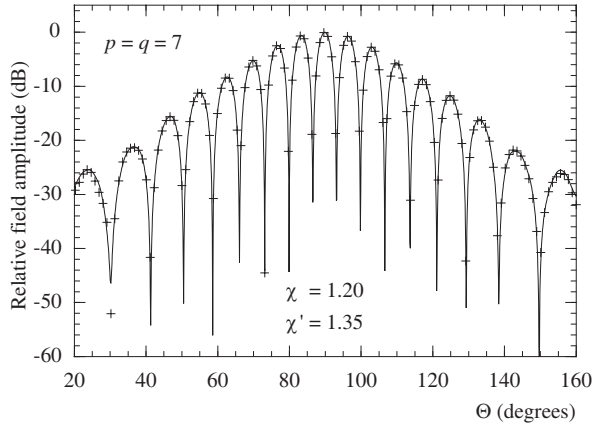

Figure 8. H-plane pattern. Solid line: Direct FF measurements. Crosses: Reconstructed from NF data acquired via helicoidal scanning.
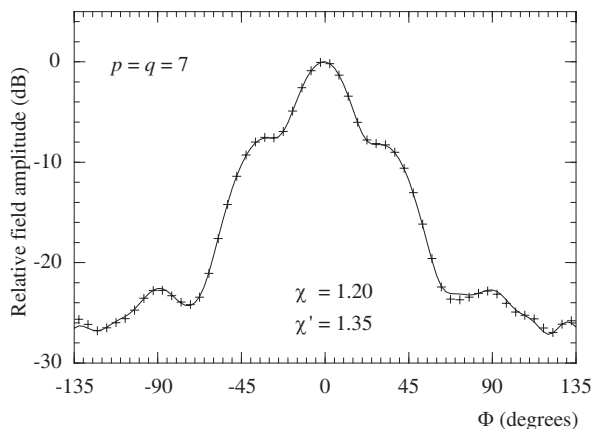

Figure 9. E-plane pattern. Solid line: Reference. Crosses: Reconstructed from NF data acquired via helicoidal scanning.

acquired helicoidal NF data with that obtained from the data directly measured on the classical cylindrical grid, whereas, in Fig. 11, the H-plane pattern obtained from helicoidal measurements is compared with that directly measured in the FF zone. The same comments done for Figs. 7 and 8 hold.

Figure 10. H-plane pattern. Solid line: Reference. Crosses: Reconstructed from NF data acquired via helicoidal scanning.
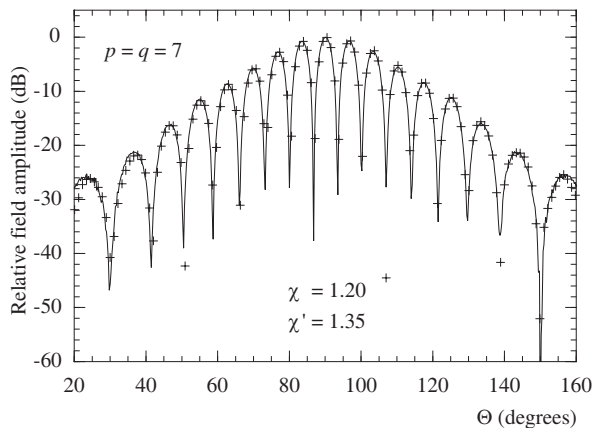
Figure 11. H-plane pattern. Solid line: Direct FF measurements. Crosses: Reconstructed from NF data acquired via helicoidal scanning.

It is worthy to note that the number of data needed by the described NF-FF transformation with helicoidal scan is 1620,

remarkably less than that (5796) required by the traditional NF cylindrical scanning and the NF helicoidal scanning technique [16] to cover the same measurement zone. This number is comparable with that (1904) needed by the nonredundant NF-FF transformation with cylindrical scanning [20].

4. CONCLUSION

An experimental validation of the NF-FF transformation with helicoidal scanning, which makes use of the prolate ellipsoidal modelling of the AUT [13], has been provided in this paper. Such a modelling allows one to efficiently fit electrically long antennas. It is so possible to significantly reduce the number of the needed NF data and, as consequence, of the required measurement time. Moreover, the employed AUT modelling enables one to consider measurement cylinders having diameter less than the antenna maximum size, thus remarkably reducing the error related to the truncation of the scanning zone.

ACKNOWLEDGMENT

REFERENCES

1. Yaghjian, A. D., "An overview of near-field antenna measurements," *IEEE Trans. Antennas Propagat.*, Vol. 34, 30–45, January 1986.
2. Bucci, O. M., C. Gennarelli, G. Riccio, and C. Savarese, "Probe compensated NF-FF transformation with helicoidal scanning," *Journal of Electromagnetic Waves and Applications*, Vol. 14, No. 4, 531–549, 2000.
3. Bucci, O. M., C. Gennarelli, G. Riccio, and C. Savarese, "Nonredundant NF-FF transformation with helicoidal scanning," *Journal of Electromagnetic Waves and Applications*, Vol. 15, No. 11, 1507–1519, 2001.
4. Bucci, O. M., F. D'Agostino, C. Gennarelli, G. Riccio, and C. Savarese, "Probe compensated FF reconstruction by NF planar spiral scanning," *IEE Proc. — Microw., Ant. Prop.*, Vol. 149, 119–123, April 2002.

5. Bucci, O. M., F. D'Agostino, C. Gennarelli, G. Riccio, and C. Savarese, "NF-FF transformation with spherical spiral scanning," *IEEE Antennas Wireless Propagat. Lett.*, Vol. 2, 263–266, 2003.

6. D'Agostino, F., F. Ferrara, C. Gennarelli, G. Riccio, and C. Savarese, "Directivity computation by spherical spiral scanning in NF region," *Journal of Electromagnetic Waves and Applications*, Vol. 19, 1343–1358, 2005.

7. D'Agostino, F., C. Gennarelli, G. Riccio, and C. Savarese, "Theoretical foundations of near-field-far-field transformations with spiral scannings," *Progress In Electromagnetics Research*, PIER 61, 193–214, 2006.

8. Yaccarino, R. G., L. I. Williams, and Y. Rahmat-Samii, "Linear spiral sampling for the bipolar planar antenna measurement technique," *IEEE Trans. Antennas Propagat.*, Vol. 44, 1049–1051, July 1996.

9. Bucci, O. M., C. Gennarelli, and C. Savarese, "Representation of electromagnetic fields over arbitrary surfaces by a finite and nonredundant number of samples," *IEEE Trans. Antennas Propagat.*, Vol. 46, 351–359, March 1998.

10. Bucci, O. M., C. Gennarelli, and C. Savarese, "Fast and accurate near-field–far-field transformation by sampling interpolation of plane-polar measurements," *IEEE Trans. Antennas Propagat.*, Vol. 39, 48–55, January 1991.

11. Gennarelli, C., G. Riccio, V. Speranza, and C. Savarese, "Fast and accurate interpolation of radiated fields over a cylinder," *Progress In Electromagnetics Research*, PIER 8, 349–375, 1994.

12. Leach, Jr., W. M. and D. T. Paris, "Probe compensated NF measurements on a cylinder," *IEEE Trans. Antennas Propagat.*, Vol. 21, 435–445, July 1973.

13. D'Agostino, F., F. Ferrara, C. Gennarelli, R. Guerriero, and M. Migliozzi, "Near-field-far-field transformation technique with helicoidal scanning for elongated antennas," *Progress In Electromagnetics Research B*, Vol. 4, 249–261, 2008.

14. D'Agostino, F., F. Ferrara, C. Gennarelli, R. Guerriero, and M. Migliozzi, "The unified theory of near-field-far-field transformations with spiral scannings for nonspherical antennas," *Progress In Electromagnetics Research B*, Vol. 14, 449–477, 2009

15. D'Agostino, F., F. Ferrara, C. Gennarelli, R. Guerriero, and M. Migliozzi, "An effective NF-FF transformation technique with planar spiral scanning tailored for quasi-planar antennas," *IEEE Trans. Antennas Propagat.*, Vol. 56, 2981–2987, September 2008.

16. Costanzo, S. and G. D. Massa, "Far-field reconstruction from phaseless near-field data on a cylindrical helix," *Journal of Electromagnetic Waves and Applications*, Vol. 18, No. 8, 1057–1071, 2004.

17. Costanzo, S. and G. D. Massa, "Near-field to far-field transformation with planar spiral scanning," *Progress In Electromagnetics Research*, PIER 73, 49–59, 2007.

18. Sten, J. C.-E. and E. A. Marengo, "Transformation formulas for spherical and spheroidal multipole fields," *AEÜ Int. J. Electron. Commun.*, Vol. 61, No. 4, 262–269, 2007.

19. Bucci, O. M., G. D'Elia, and M. D. Migliore, "Advanced field interpolation from plane-polar samples: Experimental verification," *IEEE Trans. Antennas Propagat.*, Vol. 46, 204–210, February 1998.

20. D'Agostino, F., F. Ferrara, C. Gennarelli, G. Riccio, and C. Savarese, "NF-FF transformation with cylindrical scanning from a minimum number of data," *Microw. Opt. Technol. Lett.*, Vol. 35, 264–270, November 2002.